ATP dependence of K_{ATP} channel kinetics in isolated membrane patches from rat ventricle

C. G. Nichols, W. J. Lederer, and M. B. Cannell*

Department of Physiology, University of Maryland, Baltimore, Maryland 21201; and *Department of Pharmacology and Clinical Pharmacology, St. George's Hospital Medical School, Cranmer Terrace, London SW17 0RE, England

ABSTRACT The dependence of K_{ATP} channel activity on [ATP] has been examined in isolated membrane patches from rat ventricular myocytes. The steady-state [ATP] dependence of channel open probability could be described by a sigmoidal relationship with the k_i ([ATP] causing half-maximal inhibition of open probability) = 25 μM and Hill coefficient of 2. Description of channel open- and closed-time distributions required at least 2, and 3, time constants, respectively. Long open-channel lifetimes decreased with [ATP]; unconditional mean channel closed-times increased with [ATP]. Step decrease (jump) in bathing [ATP] resulted in a delay (of up to hundreds of milliseconds) followed by a pseudo-exponential rise of current (with a time constant of up to hundreds of milliseconds). The time course of channel current after changes of [ATP] (or the ATP-analogue AMP-PNP) was shown to be predominantly determined by the time course of diffusion into the tip of the electrode and to the membrane. This time course of diffusion of ATP into the pipette tip had to be taken into account when analyzing the current response to [ATP] steps. Several possible kinetic models of the ATP-dependent regulation of channel activity were considered. Adequate explanation of the data required a model with sequential ATP-binding sites. The model can account for the time course of channel opening after steps of [ATP], as well as for the steady-state dependence of P_0 on [ATP]. The model predicts [ATP]-dependent closed and open lifetimes as were observed experimentally.

INTRODUCTION

A novel class of K^+-channels, inhibited by low concentrations of intracellular ATP, was first identified in heart muscle (Noma, 1983) and has since been observed in skeletal and smooth muscle, pancreatic β-cells, and brain (see Ashcroft, 1988). These channels are now recognized as important mediators of potential therapies for certain disease states: in the pancreas, channel inhibition by sulfonylureas is an antidiabetic mechanism; in smooth muscle, channel opening by drugs such as pinacidil is antihypertensive (Weston and Abbott, 1987).

The mechanism by which ATP regulates the activity of K_{ATP} channels has been the subject of much investigation. There is general agreement that these channels are inhibited by the binding of ATP to the channel without hydrolysis of ATP (but see Ribalet, Ciani, and Eddlestone, 1989; Nichols and Lederer, 1991). Measurement of single channel kinetics has been severely hampered by the rundown of channel activity that follows patch isolation (Trube and Hescheler, 1984). The development of the oil-gate chamber by Qin and Noma (1988) allows step changes (jumps) of [ATP] at the tip of a patch electrode and has been used to provide an alternate means of studying the ATP dependence of K_{ATP} channel kinetics (Qin, Takano, and Noma, 1989). In combination with measurements of single-channel dwell-time distributions, such measurements have been used to develop a mechanistic model of ATP binding to the channel. The model of Qin et al. (1989) can reproduce some of the features of the ATP dependence of cardiac K_{ATP} channel kinetics (Qin et al., 1989). There are, however, at least two major shortcomings of this model: (*a*) this model does not explain the long latency to channel opening that is observed on removal of ATP (Qin and Noma, 1988; Lederer and Nichols, 1989; Qin et al., 1989); and (*b*) other studies have shown that cardiac K_{ATP} channels require a Hill coefficient of ~2 to fit the steady-state [ATP] dependence of channel activity (Noma, 1983; Findlay, 1988; Lederer and Nichols, 1989). The model of Qin et al. (1989) predicts that the steady-state [ATP] dependence of channel opening should have a Hill coefficient of 1. To increase the steepness of the relationship, the ATP unbinding reaction has been suggested to be [ATP] dependent (Qin et al., 1989).

In the preceding paper, we have described limitations in the use of isolated membrane patches to measure the kinetics of ligand-channel interaction (Cannell and Nichols, 1991). In this study, we have taken such limitations into account in reexamining the kinetics of K_{ATP} channel gating by ATP. The results suggest that the delay (or lag) observed in oil-gate experiments on K_{ATP}

Dr. Nichols' present and permanent address is Department of Cell Biology and Physiology, Box 8228, Washington University School of Medicine, 660 South Euclid Avenue, St. Louis, MO 63110.

0006-3495/91/11/1164/14 $2.00

channels is principally due to the diffusion-limited exit of ATP from the patch pipette. The results are used to develop a new model for K_{ATP} channel gating which accounts for the steady-state [ATP] dependence of channel activity without requiring [ATP] dependence of ATP unbinding.

METHODS

General

Single ventricular myocytes were obtained from adult rat hearts by established enzymatic dissociation techniques (see Lederer and Nichols, 1989). Experiments were performed at room temperature, in an oil-gate chamber (Qin and Noma, 1988), described in Lederer and Nichols (1989), which allowed step changes in the solution bathing the patch pipette.

Microelectrodes (5–40 MΩ) were pulled from filamented borosilicate glass (1.5 mm o.d., No. 1B150F-6; WPI Inc., New Haven, CT) on a horizontal puller (BB-CH Mechanex, Geneva, Switzerland). Micropipettes were sealed onto cells by applying light suction to the rear of the pipette, and inside-out patches were obtained by lifting the electrode and then passing the electrode tip through the oil-gate, which caused the patch of membrane to be excised from the cell.

Solutions

The standard pipette (extracellular) solution used throughout these experiments had the following composition (mM): NaCl, 140; KCl, 4; $CaCl_2$, 1; Na-Hepes 5. The pH was 7.2. The standard bath (intracellular) solution contained (mM): KCl, 140; K-Hepes, 10; K-EGTA, 1. The solution pH was 7.25. Additions to this solution are described in Results. ATP was added as the K^+ salt; AMP-PNP, used in Fig. 5, was added as the Li^+ salt. Mg^{2+} was absent from all solutions.

Data collection and analysis

Patch-clamp currents were measured using a Dagan model 8900 patch clamp (Dagan Corp., Minneapolis, MN) with a 10-GΩ headstage, and filtered at 1 kHz or 10 kHz. Signals were digitized at 22 kHz (Neurocorder; Neurodata, New York) and stored on video tape. Multichannel data was replayed through a 1 or 5 kHz 8-pole Bessel filter and digitized at 20 kHz by a microcomputer (Compaq Computer Corp., Houston, TX).

Parameter fitting and simulations

The time course of K^+ and of ATP concentration changes at the membrane in response to step changes of their concentration at the tip of the pipette was estimated using the model described in the preceding paper (Cannell and Nichols, 1991). Briefly, the pipette was modelled as a right cone, with the membrane patch situated some distance from the tip opening. The diffusion of solutes into and out of the pipette was calculated with a nonlinear, finite element method. The equations describing the flux of solute between elements and solute binding to the channel were integrated with a program for the solution of stiff differential equations (FACSIMILE; Chance et al., 1977). This program also allowed least-squares fitting of model parameters to experimental records.

Channel activity was simulated with a modified version of the Turbo C program described in Cannell and Nichols (1991) which incorporated multiple ATP bound states. Further details of the model are given in the text where appropriate.

RESULTS

Measurement of ATP-dependent K_{ATP} channel activity in cardiac membrane patches

When a patch containing K_{ATP} channels is excised from the cell, into a solution containing zero ATP, channel activity is initially very high, with the open probability (P_0) ~ 0.95. However, the K_{ATP} channel activity does not remain constant but decreases with time after isolation. This phenomenon, termed rundown (Trube and Hescheler, 1984), is illustrated in Fig. 1 *A*, which shows the current in a membrane patch containing seven active channels. At the beginning of the record, immediately after excising the patch into the zero ATP solution, P_0 is

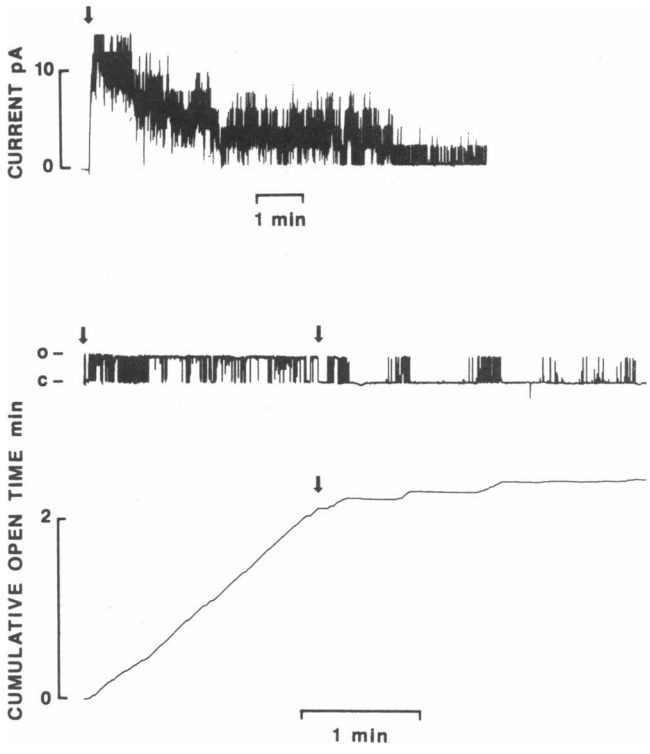

FIGURE 1 Rundown of K_{ATP} channel activity in cardiac membrane patches. (*A*) (*top*) Current (at a holding potential of 0 mV) in a membrane patch after isolation (at *arrow*). Initially, seven channels are active. The activity declines over several minutes. (*B*) (*bottom*) Membrane current in a patch containing only one channel after isolation from the cell (*above*) and the time integral of membrane current, the slope of which is a reflection of cumulative open time (*below*). The patch was isolated at the first arrow. The second arrows mark a step change in channel open probability.

high, but declines to a low level within 10 min of isolation. This phenomenon seriously complicates the determination of dwell-time distributions. However, in patches containing a single active K_{ATP} channel, such rundown apparently occurs as a sudden decrease in channel open probability. A convenient measure of channel open probability is provided by the time integral of membrane current, and as shown in Fig. 1 *C*, the time integral (cumulative open time) increases approximately linearly up to the point indicated by the arrow. Thereafter, the integral increased more slowly and discontinuously. This behavior is reminiscent of the 'moding' behavior of other channel types (Hess, Lansman, and Tsien, 1984). We speculate that the step change in P_0 may arise from a quantal dephosphorylation of the channel (Takano, Qin, and Noma, 1990). However, in order to avoid the complications of such changes in behavior in the analysis of channel activity, we have limited our analysis of experimental data to that obtained immediately after patch isolation, before the step change of channel behavior occurs in single channels, or before significant rundown of multichannel patch activity had occurred. If rundown of multichannel patch activity exceeding 15% of initial activity was detected, then the experimental records were not used.

Steady-state nucleotide dependence of K_{ATP} channel open probability in inside-out patches

Fig. 2 *A* shows typical current records from an experiment using the oil-gate technique to change rapidly the solution bathing the intracellular surface of the membrane patch. At a holding potential of 0 mV, with a physiological K^+ gradient across the membrane (see Methods), the single channel current is 1.85 pA with a chord conductance of 23 pS (Lederer and Nichols, 1989). In zero [ATP], the maximum channel opening probability was very high, and in this experiment the patch contained 10 active channels. The pipette was

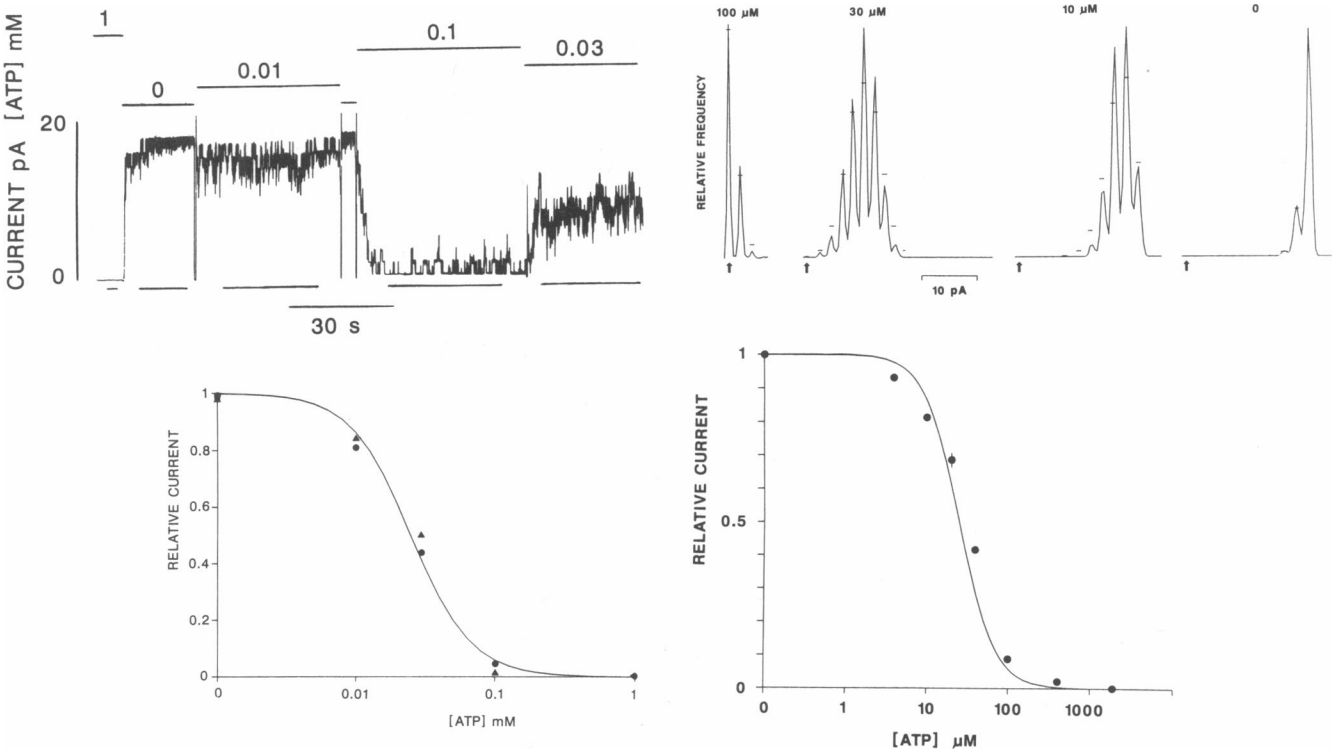

FIGURE 2 Steady-state ATP dependence of K_{ATP} channel open probability in inside-out patches. (*A*) (*top left*) Typical current record from an experiment using the oil-gate technique. A patch was sequentially exposed to 1, 0, 0.01, 0, 0.1, and 0.03 mM [ATP]. (*B*) (*top right*) Amplitude histograms of the data from periods indicated together with predicted distributions from best estimates from binomial distribution of 10 identical and independent channels (*dashes*). (*C*) (*bottom left*) Patch current during the periods indicated by bars in *A* (normalized to the current in zero ATP) plotted as a function of [ATP] (*triangles*), together with the predicted open probability (from *B*) as a function of [ATP] (*circles*). The solid line is drawn according to Equation 1 in the text with $H = 1.8$ and $k_i = 27$ μM. (*D*) (*bottom right*) Average steady-state ATP dependence of channel activity. Points show means±SEM (where SEM larger than the graphic symbols), for $n = 4$–18 experiments in each case. The solid lines are fitted with $H = 2.0$ and $k_i = 25$ μM.

moved sequentially into 0.01, 0, 0.1, and 0.3 mM ATP. Amplitude histograms were constructed from the data in Fig. 2 *A* and are shown in Fig. 2 *B*. There is good agreement between the observed current amplitude distribution at each [ATP] and that expected for 10 identical and independent channels. The ATP dependence of channel opening probability obtained from fitting the current amplitude histograms is shown in Fig. 2 *C* (*circles*) as well as the ATP dependence of the mean patch current normalized to that measured in zero ATP (*triangles*). The solid line is drawn according to the equation:

$$I = 1/(1 + [\mathrm{ATP}/k_i]^H), \quad (1)$$

where I = relative current, or open probability; ATP = [ATP]; k_i = [ATP] causing half-maximal inhibition of channel opening; H = Hill coefficient. Both sets of data are quite well described by $H = 1.8$, and $k_i = 27$ μM. The good agreement between the mean patch current and open probability (calculated from fitting a binomial distribution) suggested that the mean patch current can provide a convenient measure of P_0. Although there was some variation of k_i in different patches (between 10–50 μM), the pooled data (from 4 to 18 patches per point) was well described by $k_i = 25$ μM and $H = 2$ (Fig. 2 *D*).

We have also measured the dependence of channel activity on the nonhydrolyzable ATP analogue adenylylimidodiphosphate (AMP-PNP; Lederer and Nichols, 1989). This dependence was well described by $k_i = 60$ μM and $H_{AMPPNP} = 2$. The k_i was therefore 2.4-fold higher than the k_i for inhibition by ATP.

Dependence of K_{ATP} channel dwell-time distributions on [ATP].

Dwell-time distributions were constructed from data obtained during the first minute after patch isolation in order to avoid the problem of contamination of the data by channel run down, as described above. Fig. 3 *A* shows typical current records from single channel experiments. Fig. 3 *B* shows typical dwell-time distributions at three different [ATP]. Open-time distributions were constructed from single openings in patches containing one to five channels. Only patches containing a single active channel (in zero ATP) were used to measure channel closed times. At each [ATP], at least three time constants would be required to fully describe the closed-time distribution, whereas open-time distributions could be reasonably well described by two time constants. Fig. 3 *C* shows the [ATP] dependence of fitted open-time constants. The fast open-time constant was relatively [ATP] independent, however, the slower time constant exhibited clear [ATP] dependence, decreasing as [ATP] increased. The long mean open time was ~50% reduced at [ATP] of 10–50 μM (Fig. 3 *B*). The slope factor appeared to be less than that observed for the [ATP] dependence of channel open probability (Fig. 2), implying that the channel closed times must also be [ATP] dependent. This was found to be the case, as shown in Fig. 3 *C*. Channel closed time clearly increased as [ATP] increased, but the difficulty in obtaining single channel patches precluded a more detailed analysis at this time.

Time course of channel response to a change of [ATP]

In multichannel patches, the kinetics of the change in P_0 in response to a step change (jump) in [ATP] was examined. As the patch was moved from zero ATP to 1 mM ATP, P_0 decreased to low levels within 100 ms (see Fig. 4 *A*). When the patch was reexposed to the zero ATP solution, several hundred milliseconds elapsed before the channel activity was restored. It is notable that the increase in channel activity on returning to a zero ATP solution is not well described by a single exponential, but instead there appears to be a delay before the increase in channel activity takes place. As reported by Qin et al. (1988), this delay (lag) decreased as the preconditioning [ATP] was reduced (Fig. 4 *B*). Although such a relationship might arise from an [ATP] dependence of ATP unbinding, as suggested by Qin et al. (1989), an alternative explanation would be that the time course of diffusion of ATP out of the pipette was affecting the time course of channel activity.

Qin and Noma (1988) estimated the time course of diffusion of [ATP] to and from the membrane by measuring the time course of patch leakage current after a step change in the bathing [K^+]. In view of the uncertainty as to the exact pathway(s) through which the leakage current passes, we have measured the time course of the change in open channel current through K_{ATP} channels themselves after step changes (jumps) of bath [K^+] from 4 to 150 mM and back to 4 mM (Fig. 4 *A*). This current change reflects the time course of change in electrochemical driving force for K^+. In Fig. 5 *B* we have plotted the half-time for change in current after a step change of ATP from zero to 1 mM (*circles*) and back to zero (*triangles*) against the half-time of change in current on stepping K^+ from 140 to 4 mM in the same patch. Significantly, there is a correlation in each case ($r^2 = 0.88$ and 0.93, respectively).

Using the observed relationship between steady-state open channel current and [K^+] (Cannell and Nichols, 1991), we transformed the time course of change in current to that of [K^+]. The time course of change in [K^+] was then used to estimate the distance of the membrane from the pipette tip (L_{PIP}) having optically measured the half-angle of taper of the pipette tip (θ)

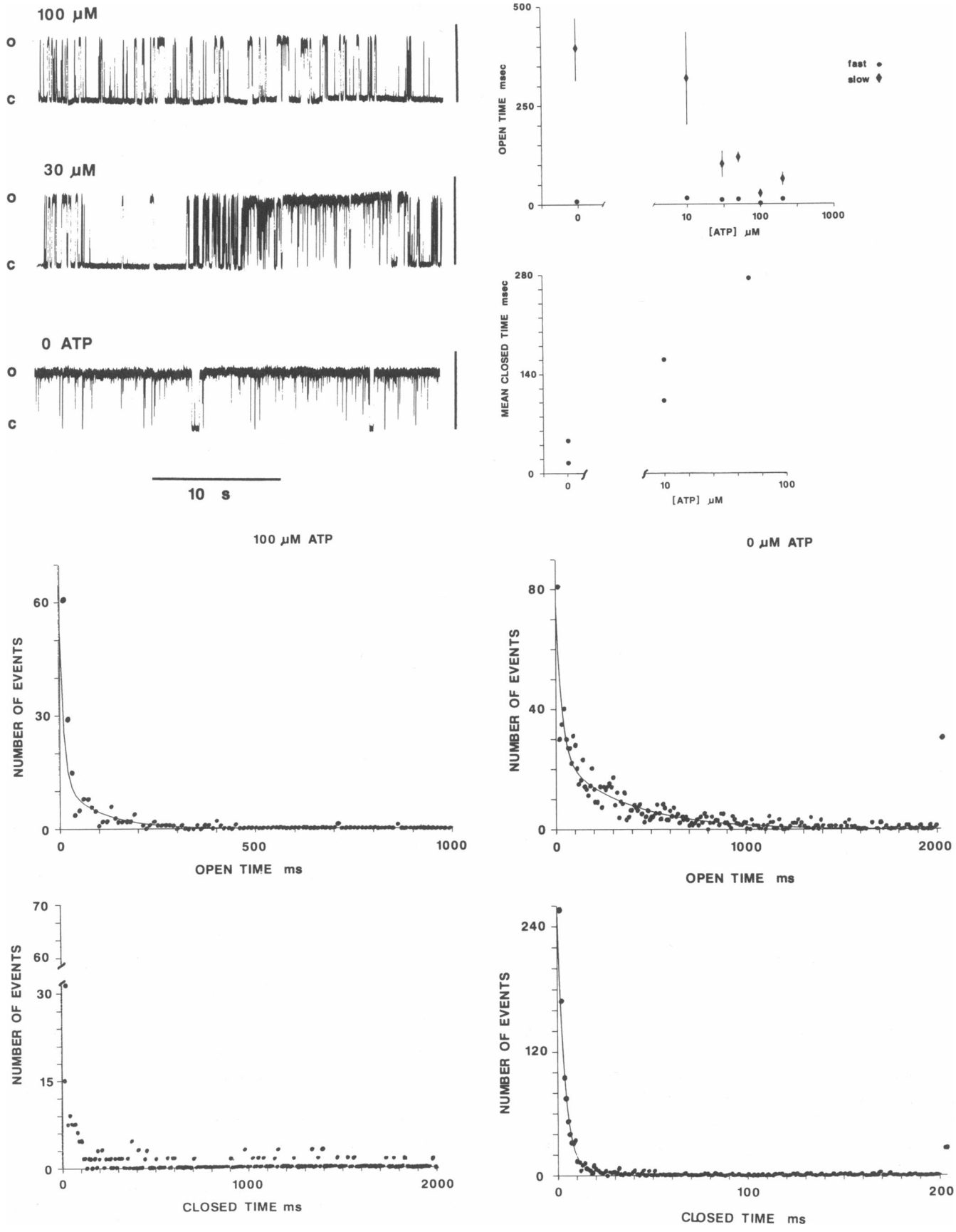
100 µM
o
c
30 µM
o
c
0 ATP
o
c
10 s
OPEN TIME msec
500
250
0
fast
slow
0
10
100
1000
[ATP] µM
MEAN CLOSED TIME msec
280
140
0
0
10
100
[ATP] µM
100 µM ATP
NUMBER OF EVENTS
60
30
0
0
500
1000
OPEN TIME ms
0 µM ATP
NUMBER OF EVENTS
80
40
0
0
1000
2000
OPEN TIME ms
NUMBER OF EVENTS
70
60
30
15
0
0
1000
2000
CLOSED TIME ms
NUMBER OF EVENTS
240
120
0
0
100
200
CLOSED TIME ms

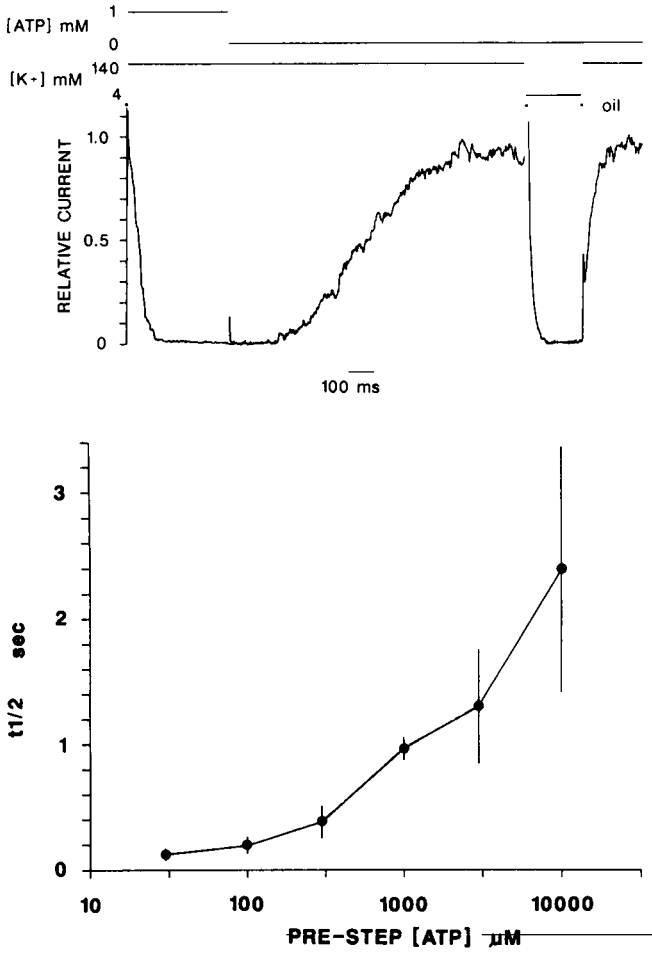

FIGURE 4 Time course of channel response to step changes of [ATP] and of [K^+]. (*A*) (*top*) Record of patch current with steps of ATP from zero to 1 mM and from 1 mM to zero, and of K^+ from 140 to 4 mM and back to 140 mM. (*B*) (*bottom*) The dependence of $t_{1/2}$ of current increase (after a step to zero ATP) on prestep [ATP].

and tip radius (R_{TIP}) after the experiment (Cannell and Nichols, 1991). There was considerable variation in the calculated depth of the patch from the pipette tip. In eight experiments, the calculated patch depth varied between 3.2 and 23 μm (7.5 ± 0.7 μm, mean±SE). In the same patches, we also applied a least-squares analysis similar to that used by Qin et al. (1989), which assumed that the time course of change in channel current after a step from 1 mM to zero ATP could be described by an exponential after a lag (see Fig. 6 *B*). Fig. 6 *C* is a plot of the lag and the time constant versus the calculated patch depth. There was clearly a dependence of both the lag and the time constant on the patch depth. In each case the time was proportional to the square of the patch depth. The simplest explanation of this observation would be that the time course of diffusion of ATP out of the patch pipette was dominating the observed time course of change in channel activity.

The delay to channel opening is present for other blocking nucleotides

If the delay to channel opening (lag) is due to diffusion (as suggested by the above results), then a delay should exist for all other blocking nucleotides. However, Qin et al. (1989) reported that although a delay was observed with ATP, no delay was observed on channel opening after removal of AMP-PNP. We have reexamined the time course of channel unblock on removal of both AMP-PNP and ATP in the same patches. Fig. 7 *A* shows an original record of the patch current on removal of ATP and AMP-PNP. It is clear that the time course for both blockers is similar although the lag is somewhat smaller when AMP-PNP is removed compared with the removal of ATP. The results ~~of a number~~ of similar experiments are summarized in Fig. 7 *B*. The half-time for current increase on removal of ATP is proportional to the half-time for the increase on removal of AMP-PNP[1] (see page 1172). A correlation between the $t_{1/2}$ on removal of ATP and the $t_{1/2}$ on removal of blocking doses of ADP was also observed (data not shown). This is exactly as expected for a diffusion-limited process, because it demonstrates that, after removal of blocking nucleotide, a lag before channel opening is not intrinsic to recovery from ATP inhibition (Qin et al., 1989).

Reconstruction of the kinetics of changes in channel open probability

Because the time course of channel opening seems to be limited by the time course of diffusion of nucleotides out

FIGURE 3 Dependence of K_{ATP} channel open- and closed-time distributions on [ATP]. (*A*) (*top left*) Experimental records of single-channel activity at indicated [ATP]. (*B*) (*bottom left* and *right*) Typical open- and closed-time distributions at [ATP] = 0 and 100 μM. Open-time distributions were constructed from single openings in patches containing one to five channels. At least three time constants were required to fully describe the closed-time distribution (at ATP = 0 μM), whereas open-time distributions were reasonably well described by two time constants (at ATP = 0 and 100 μM). In each case, the number of out-of-range unbinned events are marked at right of graph. (*C*) (*top right*) [ATP] dependence of fitted fast (*circles*) and slow (*diamonds*) open-time constants (*above*), and unconditional mean closed times (*below*).

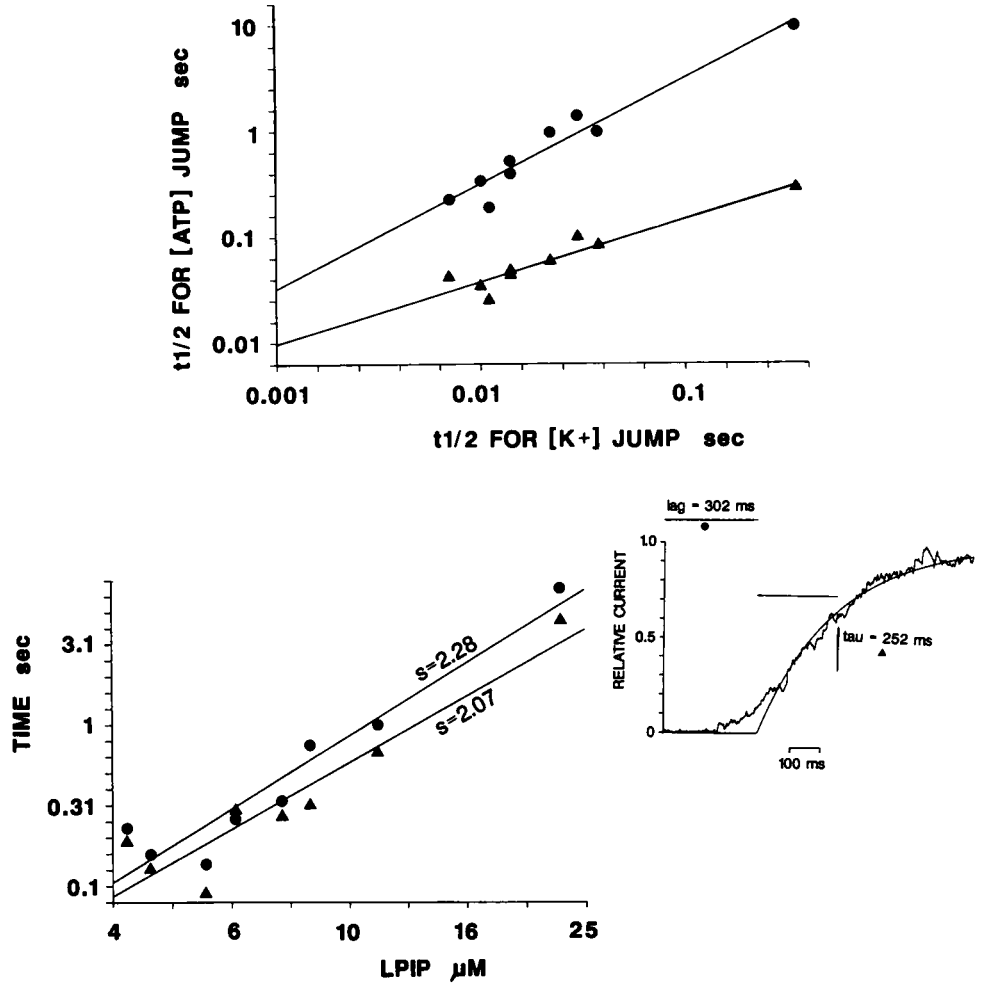

FIGURE 5 The dependence of current recovery on diffusion. (*A*) (*top*) Graph showing the $t_{1/2}$ of channel current change after step changes of ATP (from 1 mM to zero (*circles*) and from zero to 1 mM (*triangles*)) versus the $t_{1/2}$ of channel current change after a step change of K^+ (from 140 to 4 mM). Points are from individual experiments. (*B*) (*bottom*) Graph showing lag time (lag; *circles*) and time constant (tau; *triangles*) of current change (as fitted in *inset*) for step decrease of ATP from 1 mM to zero versus patch depth (calculated as described in Cannell and Nichols, 1990) for the same set of data as in *A*.

of the pipette, we have taken the approach described in Cannell and Nichols (1991) in an attempt to extract the rate constants for channel—nucleotide interaction. As described above (cf. Fig. 4), we measured, in the same patch, the time course of current change after step changes of $[K^+]$ and of [ATP] from 1 mM to zero, and back to 1 mM. Having used the $[K^+]$-jump data to calculate the patch depth (see above), the time course of change in [ATP] at the membrane ws calculated (given a diffusion coefficient of 4.5×10^{-6} cm^2/s as compared with 1.83×10^{-5} cm^2/s for K^+; Qin and Noma, 1988). The time course of channel opening was then simulated by adopting various kinetic models, and kinetic parameters for the models fitted to the experimental data (see Cannell and Nichols, 1991).

In increasing complexity, the models we have considered are:

$$C_{ATP}—C—O \quad [1]$$

$$C—O—C_{ATP} \quad [2]$$

$$C—O\begin{matrix}\diagup Cl_{ATP}\\ \diagdown C2_{ATP}\end{matrix} \quad Cl_{ATP}C2_{ATP} \quad [3]$$

$$C—O—Cl_{ATP}—Cl_{ATP\text{-}ATP} \quad [4]$$

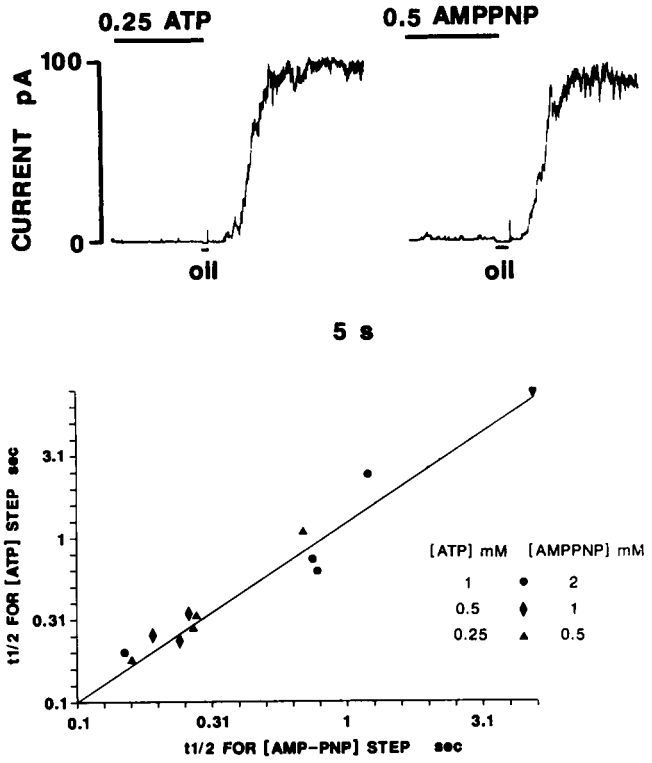

FIGURE 6 The delay to channel opening is present for other blocking nucleotides. (*A*) (*top*) Record of patch current after step decrease of [ATP] from (0.25 mM to zero), and of [AMP-PNP] (from 0.5 mM to zero) in the same patch. (*B*) (*bottom*) Plot of $t_{1/2}$ of current recovery after step decreases of ATP to zero versus the $t_{1/2}$ of recovery after step decreases of AMP-PNP to zero in the same patches (The prestep [ATP] and [AMP-PNP] are indicated).

$$C{-}O{-}C1_{ATP}{-}C1_{ATP\text{-}ATP}{-}C1_{ATP\text{-}ATP\text{-}ATP} \quad [5]$$

$$C{-}O \begin{cases} C1_{ATP} \\ C1_{ATP}C2_{ATP} \\ C2_{ATP} \end{cases} \begin{cases} C1_{ATP\text{-}ATP} \\ C1_{ATP\text{-}ATP}C2_{ATP} \\ C1_{ATP}C2_{ATP\text{-}ATP} \\ C2_{ATP\text{-}ATP} \end{cases} \begin{cases} C1_{ATP\text{-}ATP}C2_{ATP\text{-}ATP} \end{cases} \quad [6]$$

Schemes 1 and 2 are the simplest schemes which might describe the channel activity. However, these schemes can be rejected by inspection. Scheme 1 predicts ATP-independent open lifetime and scheme 2 predicts ATP-independent closed time. Neither condition is met by the single channel data (Fig. 3). In addition, these schemes predict a Hill coefficient of 1 in the dose-response curve to ATP which is also not observed (Fig. 2).

The next schemes in increasing complexity are 3 and 4. Scheme 3 and other schemes with more nonsequential ATP binding sites all predict Hill coefficients of ~1.5. Sequential ATP-binding sites predict higher Hill coefficients. Scheme 4 consists of sequential 2-site ATP binding and predicts a Hill coefficient of 2, and so might be able to explain the experimental data. However, this model consistently predicted too small a delay to the onset of channel opening and too slow a subsequent rise in channel activity when attempting to fit experimental records with a jump of [ATP] to zero. Increasing the complexity of this model by adding further sequential ATP binding states after $C1_{ATP\text{-}ATP}$ (i.e., scheme 5) would improve the fit to the kinetic data, but would be inconsistent with the measured steady-state ATP-dependence of P_o because such models predict Hill coefficients greater than 2.

Consideration of the necessity to explain an ATP dependence of P_o with $H \sim 2$ combined with a steep kinetic response led to the examination of scheme 6. This scheme is derived from scheme 4, consisting of two pairs (C1 and C2) of sequential 2-site ATP binding steps. It is assumed that the two pairs of sites are independent, thus the scheme appears complex due to the various intermediate steps leading to the fully (four) ATP-bound state. The ability of this model to fit [ATP] step change results was not substantially decreased by constraining all ATP binding rate constants to the one value and all ATP unbinding rate constants to one value. In a parameter fitting analysis, we allowed these two parameters to be varied in the patch having the fastest response to an [ATP] step (i.e., shortest calculated $L_{PIP} = 3.2$ μm), and the best fit simulated response, together with the original data is shown in Fig. 7 (*top*). The determined parameters ($k_{ATP\,on} = 250\ mM^{-1} \cdot s^{-1}$, $k_{ATP\,off} = 20\ s^{-1}$) were then used in parameter fitting runs with other data sets, fitting only the apparent patch depth (L_{PIP}) in each case. Scheme 6 with the fixed rate constants provided a good fit to the current response to [ATP] steps in these patches (e.g., Fig. 7, *middle* and *bottom*), and no consistent deviation of the simulated response from the observed response was determined, even though the apparent patch depth (L_{PIP}) varied by fivefold (from 3.2 to 18.8 μm), and the time course of channel opening varied by at least 10-fold (Fig. 7).

Monte-Carlo simulation of experimental data

The computer-fitted time course of channel opening contains no stochastic noise, and such noise is a prominent feature of the experimental data. We therefore considered it important to compare qualitatively the data that would be generated by a limited number of channels (with the rate constants calculated above) to the experimental data. Fig. 8 shows the simulated time

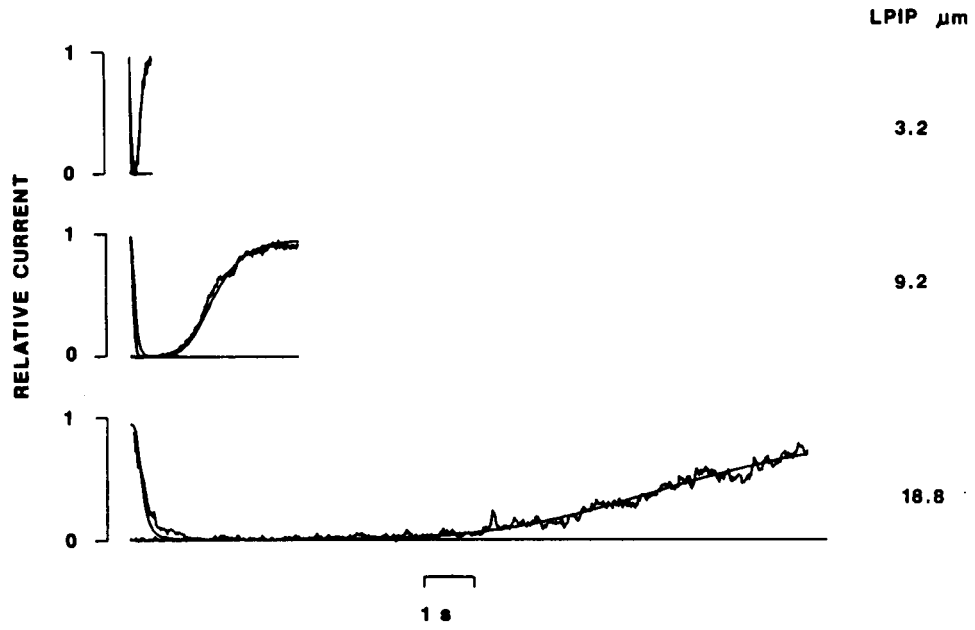

FIGURE 7 Scheme 6 can describe the patch response to [ATP] steps. Records of patch current response to step decrease of [ATP] from 1 to 0 mM and step increase from 0 to 1 mM in three different patches. In each case, the smooth curve is a fit of scheme 6 to the data with the patch depth (L_{PIP}) varied as shown. The rate constants were fixed as described in the text.

course of channel activity on lowering [ATP] from 1 mM to zero for patches containing 1 or 100 channels. As shown in Fig. 9 *A*, Scheme 4 predicts variability in the latency to first opening as was observed by Qin et al. 1989 (their Fig. 3). With 100 channels in the patch, the relative amount of stochastic noise is reduced, and the record appears very similar to the experimentally observed results. Fig. 9 shows the predicted steady-state ATP dependence of P_o together with the experimentally observed steady-state ATP dependence of channel activity. There is very good agreement between the predicted and observed results.

Fig. 10 shows simulated single channel data (F_c = 1 kHz) using Scheme 6 with the determined parameters, together with dwell-time distributions measured from such simulated data. The model predicts single exponential distributions of both open and closed times in the absence of ATP, but requires two exponentials to describe the open and closed times in the presence of ATP. The model further predicts that both unconditional mean open and closed times will be ATP dependent (Fig. 10 *C*).

DISCUSSION

We have measured, (*a*) the steady-state [ATP] dependence of channel open probability, (*b*) the steady-state

[1]As shown previously, the $t_{1/2}$ for channel unblock depends on the preconditioning [nucleotide] (Fig. 4 *B*). If the kinetics of channel unblock are rapid as compared with the time course of diffusion, then the channel activity will be approximated by the steady-state binding isotherm convolved with the time course of [nucleotide] at the membrane. Because the time course of decline of [nucleotide] can be described by an equation:

$$[\text{nucleotide}] = C_0^*(f(t)), \quad (2)$$

where C_0 is initial [nucleotide] and $f(t)$ is a function describing the diffusion of the nucleotide out of the pipette (depending on pipette geometry; Cannell and Nichols, 1991), then channel activity would be described by:

$$P_0 = 1/\{1 + [C_0(f(t))/k_i]^H\}, \quad (3)$$

where k_i is the concentration causing half-maximal block, and H = Hill coefficient. Thus, the time for half unblock of the channel will depend on both the initial concentration (C_0) of the blocking nucleotide (Fig. 4 *B*) and on the k_i and H for the blocker. By inspection of Eq. 3, if C_0 is varied in proportion to k_i, for the blockers of interest, then the half-time for channel unblock should be the same (provided H is the same for both nucleotides). The k_i for channel block by AMP-PNP is approximately twice that of ATP, with the same Hill coefficient. Thus, the half-time for channel unblock, on the basis of the above reasoning, should be the same for the experiments shown in Fig. 7 (because the initial [AMP-PNP] was chosen to be twice the initial [ATP] in each case. The data in Fig. 7 *B* appears to be consistent with this prediction, and strongly suggests that the time course of diffusion is the primary determinant of the time course of channel unblock after nucleotide removal.

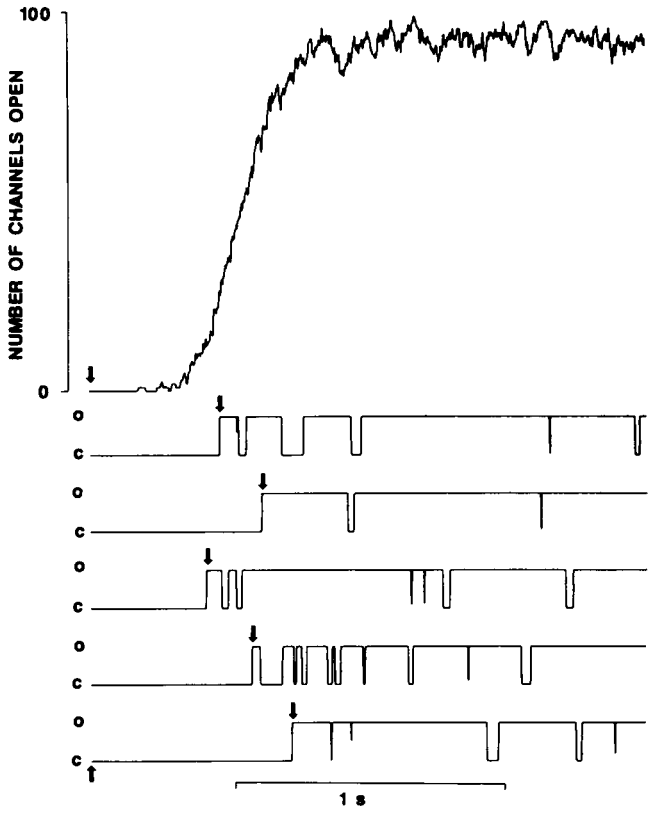

FIGURE 8 Simulated time course of channel opening with Scheme 6. Simulated time course of channel activity on lowering [ATP] from 1 mM to zero for patches containing 1 (*below*) or 100 (*above*) channels. The [ATP] is lowered to zero at the first arrow. In the single channel simulations, the first opening is marked by a second arrow.

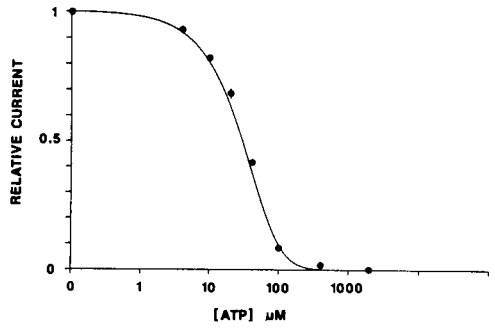

FIGURE 9 Scheme 6 can predict the steady-state ATP dependence of channel open probability. Graph showing mean (±SE) steady-state ATP dependence of channel activity (n = 4–18 in each case, redrawn from Fig. 2). Smooth curve is prediction from Scheme 6 with rate constants as given in the text.

ATP dependence of single K_{ATP} channel dwell-time distributions, and (*c*) the kinetic response to step changes of [ATP] ([ATP] jumps), in order to develop a quantitative kinetic model for cardiac K_{ATP} channel activity. In so doing, we have had to avoid the complications resulting from changes in [ATP] dependence of channel activity due to "run-down" (Trube and Heschler, 1984), and the diffusion limitations in interpreting the results of [ATP]-jump experiments (Cannell and Nichols, 1991).

Steady-state [ATP]-dependence of open probability

The [ATP] dependence of open probability (P_o) has been examined in several studies. We found that the [ATP] dependence of P_o was well described by Eq. 1, with a Hill coefficient of 2 and k_i of 25 μM. Previous studies have generally found similar for rat ventricle (Findlay, 1988; Lederer and Nichols, 1989), but higher values for guinea pig (Noma, 1983; Fan et al., 1990*a*, *b* and cat ventricular cells (Cameron et al., 1988). Although the Hill coefficient of averaged data (as in the above studies) is usually close to 2, in agreement with our data (Fig. 2), any variability in the k_i from channel to channel will mean that the Hill coefficient from averaged data represents a lower limit of the Hill coefficient of individual channels. However, we have shown that, even in a single patch containing only 10 channels, the steady-state ATP dependence of channel activity is well fit with a Hill coefficient of 2 and the channels appear to be independent without evidence of nonidentical behaviour (Fig. 2 *B* and *C*). It therefore seems likely that the true Hill coefficient of individual channels is very close to 2.

Steady-state ATP dependence of dwell-time distributions

Several studies have investigated the ATP dependence of single K_{ATP} channel dwell-times, with widely differing results. Kakei et al. (1985) suggested that at least two time constants were necessary to adequately describe both the open and closed time distributions in K_{ATP} channels from guinea pig ventricular cells, each of which appeared to be [ATP] dependent. Qin et al. (1989) measured dwell-time distributions within bursts, and determined single fast open and closed times which were [ATP] independent. The interburst intervals were not considered. However, the existence of bursts suggests that there must be more than one time constant in the open and closed time distributions. At depolarized potentials, the channel dwell-time distributions will be affected by a rapid Mg^{2+}-dependent open channel block (Horie, Irisawa, and Noma, 1987), an observation that may explain discrepancies between our results and those of earlier studies. There is also some evidence for a pure voltage (or ion flux) dependence of channel open time

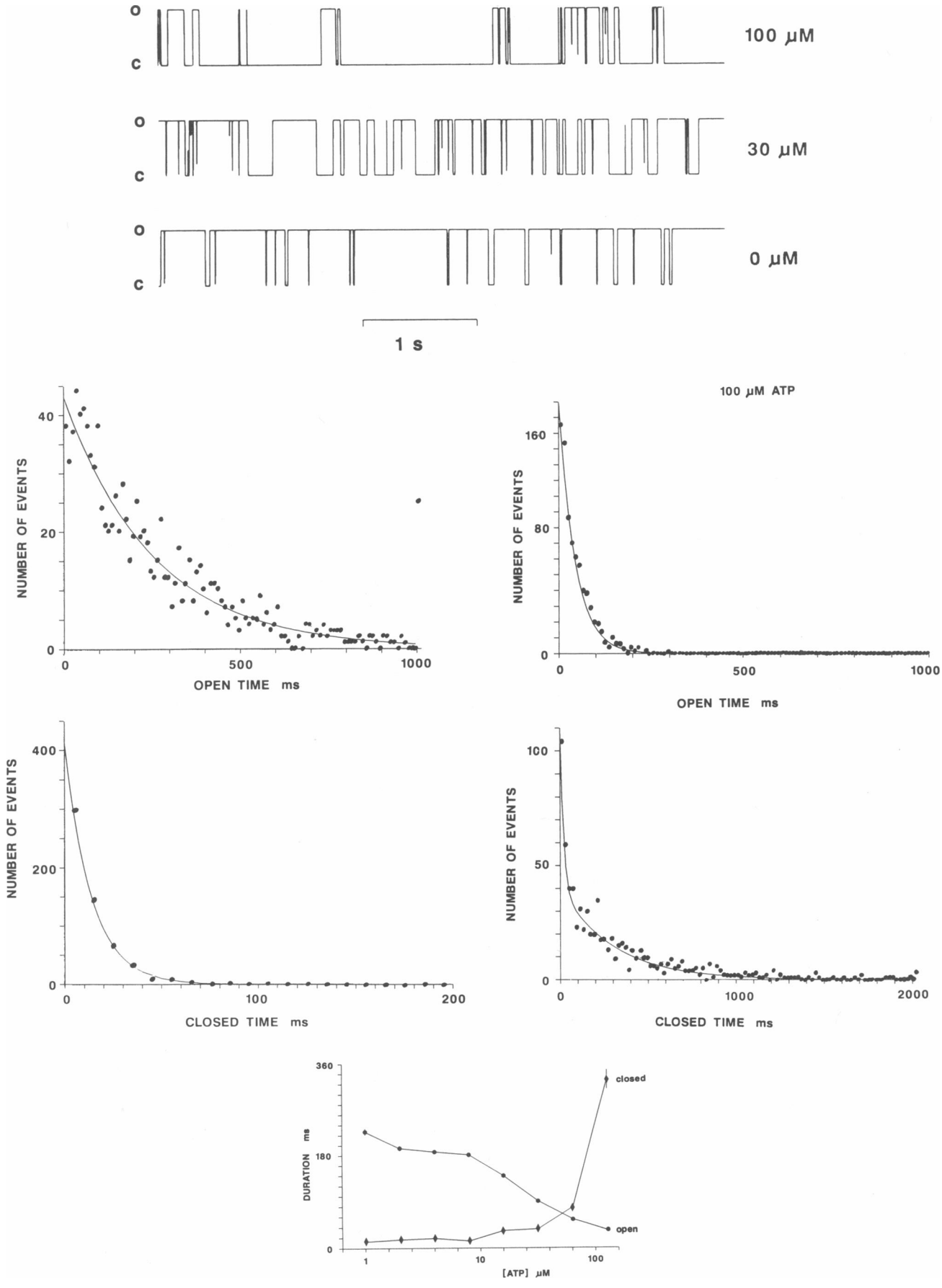
o
c
100 μM
30 μM
0 μM
1 s
100 μM ATP
NUMBER OF EVENTS
OPEN TIME ms
CLOSED TIME ms
DURATION ms
closed
open
[ATP] μM

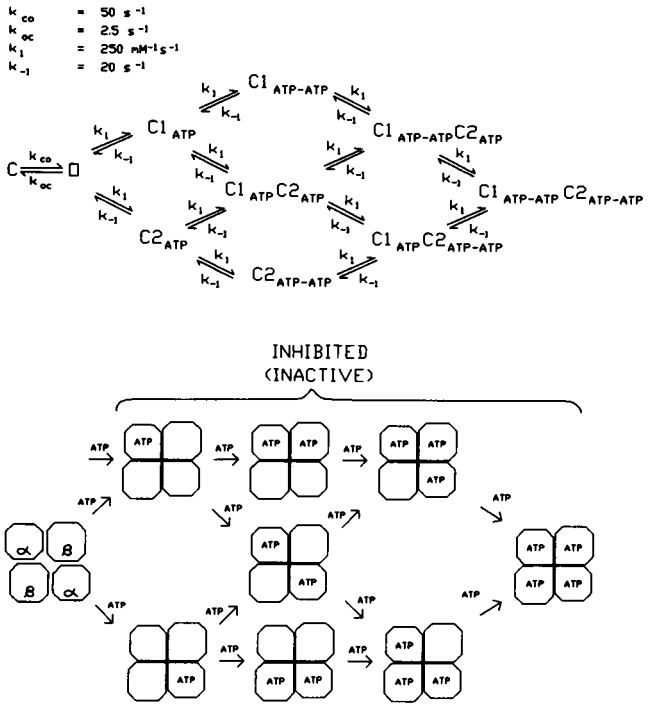

FIGURE 11 A hypothetical physical model of the K_{ATP} channel that could accommodate kinetic model Scheme 6. Channel inhibition results from binding of ATP to one of the α subunits. A subsequent ATP may then bind either the adjacent β subunit, stabilizing the inhibited channel, or to the other α subunit. The fully occupied channel would have one ATP molecule bound to each subunit.

(Zilberter et al., 1988). This phenomenon did not appear to contribute significantly to the time course of response to [ATP] jumps (Qin et al., 1989), but cannot be ruled out as another influence on channel gating. We have performed all of our experiments at a fixed voltage and K^+ driving force, in order to avoid the influence of membrane voltage or ion flux on gating. Finally, the problems introduced by channel rundown (Fig. 1) were not explicitly considered in earlier studies.

In the modeling of channel activity, we have included only 1 ATP-independent closed state and 1 ATP-independent open state (Fig. 11). This is certainly an oversimplification; we clearly observed more than one open and closed time in the absence of ATP, but the available acceptable data was so sparce that it did not warrant putting forward a more complicated model of ATP-independent activity. A detailed description of this ATP-independent activity was not required to explain the steady-state, or transient, ATP dependence of P_o, upon which we have concentrated.

The kinetic response to step changes of [ATP]

By showing a correlation between the time course of response to jumps of $[K^+]$ (which should be purely diffusion dependent), and the apparent delay (or lag) to channel opening on lowering [ATP] (Fig. 5), our results strongly suggest that the lag results primarily from diffusion-limited exit of ATP from the pipette. We therefore generally avoided the approach (Qin et al., 1989) of analyzing the K_{ATP} channel opening kinetics in terms of a lag and an exponential recovery of channel activity (but see Fig. 5 *B*). Instead, we have sought to deconvolve the kinetics of channel opening from the time course of change in [ATP]. With this approach, together with consideration of single channel data (Fig. 3), we have ruled out the simplest kinetic models (Schemes 1 and 2) that we considered to explain the data. With consideration of the steady-state [ATP] dependence of channel activity (Fig. 2), we have also excluded simple nonsequential ATP-binding schemes such as Scheme 3. Taking our analysis of [ATP] jump experiments into account, Schemes 4 or 6 seem to be minimal models to explain the data. However, Qin et al. (1989) considered that Scheme 2 could explain the data, provided that there was also ATP dependence to the unbinding of ATP. This latter feature was required to explain the apparent ATP dependence of the delay to channel opening (Fig. 4 *B*). Our results show that the ATP dependence of the delay to channel opening is in large part due to the time taken for the ATP concentration at the membrane to fall to levels where the probability of channel occupancy by ATP becomes low enough for channel opening to occur. Thus ATP-dependent unbinding of ATP is not required in order to explain the data.

A working model for K_{ATP} channel regulation by ATP

The model that we have examined in detail (Scheme 6) has not previously been considered. This model is an extension of our previous 2-site model (Scheme 4) for channel regulation (Lederer and Nichols, 1989). The model differs significantly from that (Scheme 2) pro-

FIGURE 10 Scheme 6 can predict single channel open- and closed-time distributions that are broadly consistent with experimentally measured values. (*A*) (*top*) Simulated records of single channel current from Scheme 6 (f_c = 1 kHz). (*B*) (*middle left* and *right*) Open- and closed-time distributions for 5 min of activity at two different [ATP] (fit by one open- and one closed time at 0 ATP; two open and two closed times at 100 μM ATP). (*C*) (*bottom*) Plot of mean open and closed times from simulated data (n = 30–120 events) as a function of [ATP].

posed by Qin et al. (1989). Multiple ATP bound states seems to be necessary to explain the time course of channel activity after [ATP] steps, as well as the steepness of the steady-state [ATP] dependence of channel activity. For unknown reasons (that may include the ionic composition of intra- and extracellular solutions, and membrane potential), we measured much longer open- and closed-time distributions (even with f_c = 10 kHz) than Qin et al. (1989). In our model, we have therefore chosen slower rate constants for the ATP-independent gating which reflect the dominant dwell-times measured in the absence of ATP (Fig. 3). These rate constants are important for determining single channel dwell-time distributions, but simulations showed that they are relatively unimportant in determining the kinetics of change in P_o after [ATP] jumps (which are primarily determined by the ATP-dependent steps). Scheme 6 has potentially up to 12 different ATP-binding and-unbinding rate constants. Parameter fitting with all parameters allowed to vary was unsatisfactory because it was found that the interdependence of the parameters would lead to a failure of convergence in the fitting process. We found empirically that restricting binding and unbinding rate constants to having the same values did not substantially affect the ability of the program to fit the data; we were able to fit the [ATP] jump data adequately with one ATP-binding rate constant and one ATP-unbinding rate constant. While the determined ATP-binding rate constant was faster than the rate constant determined by Qin et al. (1989), the determined ATP-unbinding rate constant was almost the same as one of the unbinding rate constants determined by Qin et al. (1989). In view of the very different kinetic schemes and method of analysis, this surprising result is probably coincidental.

Considering possible physical implications of the model, we may envisage Scheme 6 being accommodated in, for instance, a tetrameric channel made up of four monomers arranged in an αβαβ format (Fig. 11). Such an arrangement is appealing given the presumed quaternary structure of other K^+ channels for which the primary amino acid sequence is available (Tempel et al., 1988; Baumann et al., 1988). When ATP binds to either α subunit, the channel closes (or inactivates). It is not stipulated whether the ATP molecule binds to a site away from the pore and closes the channel by an allosteric change in the protein conformation, or binds in, and sterically blocks, the conducting pore itself. There is no *a priori* reason to discount this possibility, as the calculated association rate is not diffusion limited, although because ATP is negatively charged, it seems unlikely. A second ATP molecule is then free to bind either to the adjacent β subunit, or to the second α subunit. Third and fourth ATP molecules could then bind to the remaining α subunit or β subunits.

It should be borne in mind that the present modelling takes no account of the shift in open probability, and ATP dependence, that occurs as a result of rundown (Fig. 1; Trube and Hescheler, 1984; Takano et al., 1990), phosphorylation (Takano et al., 1990), or G-protein stimulation (Parent and Coronado, 1989; Kirsch et al., 1990). Future work should allow us to determine whether such shifts result from discrete changes in specific rate constants.

In the absence of ATP, the cardiac K_{ATP} channel is gated by other nucleotides (Noma, 1983; Findlay, 1988b; Lederer and Nichols, 1989). Of particular physiological significance is that in the presence of ATP, the channel activity is increased by MgADP and MgGDP (Findlay, 1988*b*; Lederer and Nichols, 1989). We have qualitatively considered this behavior in terms of a 2-site sequential binding model (Scheme 2; Lederer and Nichols, 1989) by suggesting that MgADP may bind to a site B, which stops ATP gaining access to the inhibitory site A (Lederer and Nichols, 1989). Other nucleotides, such as ADP, AMP, GTP (Lederer and Nichols, 1989), as well as potassium channel opening drugs (Thuringer and Escande, 1989; Ripoll, Lederer, and Nichols, 1990; Fan et al., 1990*a*, *b*) all interact with ATP to regulate the channel activity, either by antagonizing, or agonizing the effects of ATP. It may be that the actions of these agents can be incorporated into the model described, by binding to one or other ATP binding site, or modifying the ATP binding rate constants.

This work was supported by grants (HL-36974, to Dr. Lederer; HL-45742, to Dr. Nichols) from the National Institutes of Health, and a Grant-In-Aid (to Dr. Nichols) from the American Heart Association (Maryland Affiliate).

Received for publication 11 April 1991 and in final form 25 July 1991.

REFERENCES

Arena, J. P., and R. S. Kass. 1989. Activation of ATP-sensitive K channels in heart cells by pinacidil: dependence on ATP. *Am. J. Physiol.* 26:H2092-H2096.

Baumann, A., A. Grupe, A. Ackermann, and O. Pongs. 1988. Structure of the voltage-dependent potassium channel is highly conserved from *Drosophila* to vertebrate central nervous systems. *EMBO J.* 7:2457–2463.

Cameron, J. S., S. Kimura, D. A. Jackson-Burns, D. B. Smith and A. Bassett. 1988. ATP-sensitive K^+ channels are altered in hypertrophied ventricular myocytes. *Am. J. Physiol.* 255:H1254–H1258.

Cannell, M. B., and C. G. Nichols. 1991. The effects of pipette geometry on the time course of solution change in patch-clamp experiments. *Biophys. J.* 60:1156-1163.

Chance, E. M., A. R. Curtis, I. P. Jones, and C. R. Kirby. 1977. FACSIMILE: a computer programme for flow and chemistry simulation, and general initial value problems. Computer Science and Systems Division, Atomic Energy Research Establishment (AERE), Harwell, Oxfordshire, HMSO, London.

Colquhoun, D., and A. G. Hawkes. 1983. The principles of the stochastic interpretation of ion channel mechanisms. *In* Single Channel Recording. B. Sakmann, and E. Neher, editors. Plenum Press, New York.

Fan, Z., K. Nakayama, and M. Hiraoka. 1990*a*. Pinacidil activates the ATP-sensitive K^+ channel in inside-out and cell-attached patch membranes of guinea-pig ventricular myocytes. *Pflugers Arch.* 415: 387–394.

Fan, Z., K. Nakayama, and M. Hiraoka. 1990*b*. Multiple actions of pinacidil on adenosine triphosphate-sensitive potassium channels in guinea-pig ventricular myocytes. *J. Physiol.* 430:273–295.

Findlay, I. 1988*a*. ATP^{4-} and ATP.Mg inhibit the ATP-sensitive K^+ channel of rat ventricular myocytes. *Pflugers Arch.* 412:37–41.

Findlay, I. 1988*b*. Effects of ADP upon the ATP-sensitive K^+ channel in rat ventricular myocytes. *J. Membr. Biol.* 101:83–92.

Findlay, I., E. Deroubaix, P. Guiraudou, and E. Coraboeuf. 1989. Effects of activation of ATP-sensitive K^+ channels in mammalian ventricular myocytes. *Am. J. Physiol.* 257:H1551–H1559.

Hess, P., J. B. Lansman, and R. W. Tsien. 1984. Different modes of Ca channel gating behavior favored by dihydropyridine Ca agonists and antagonists. *Nature* (*Lond.*). 311:538–544.

Horie, M., H. Irisawa, and A. Noma. 1987. Voltage-dependent magnesium block of adenosine-triphosphate-sensitive potassium channel in guinea-pig ventricular cells. *J. Physiol.* 387:251–272.

Kakei, M., A. Noma, and T. Shibasaki. 1985. Properties of adenosine-triphosphate-regulated potassium channels in guinea-pig ventricular cells. *J. Physiol.* 363:441–462.

Kirsch, G. E., J. Codina, L. Birnbaumer, and A. M. Brown. 1990. Coupling of ATP-sensitive K^+ channels to A_1 receptors by G proteins in rat ventricular myocytes. *Am. J. Physiol.* 259:H820–H826.

Lederer, W. J., and C. G. Nichols. 1989. Nucleotide modulation of the activity of rat heart K_{ATP} channels in membrane patches. *J. Physiol.* 419:193–211.

Nichols, C. G., and W. J. Lederer. 1991. The mechanism of K_{ATP} channel inhibition by ATP. *J. Gen. Physiol.* 97:1095-1098.

Noma, A. 1983. ATP-regulated K^+ channels in cardiac muscle. *Nature* (*Lond.*). 305:147–148.

Parent, L., and R. Coronado. 1989. Reconstitution of the ATP-sensitive potassium channel of skeletal muscle. Activation by a G-protein dependent process. *Biophys. J.* 55:587*a*. (Abstr.)

Qin, D., and A. Noma. 1988. A new oil-gate concentration jump technique applied to inside-out patch-clamp recording. *Am. J. Physiol.* 255:H980–H984.

Qin, D., M. Takano, and A. Noma. 1989. Kinetics of ATP-sensitive K^+ channel revealed with oil-gate concentration jump method. *Am. J. Physiol.* 257:H1624–H1633.

Ribalet, B., S. Ciani, and G. T. Eddlestone. 1989. ATP mediates both activation and inhibition of K(ATP) channel activity via cAMP-dependent protein kinase in insulin-secreting cell lines. *J. Gen. Physiol.* 94:693–717.

Ripoll, C., W. J. Lederer, and C. G. Nichols. 1990. Modulation of ATP-sensitive K^+ channel activity and contractile behavior in mammalian ventricle by the potassium channel openers cromakalim and RP49356. *J. Pharmacol. Exp. Ther.* 255:429–435.

Takano, M., D. Qin, and A. Noma. 1990. ATP-dependent decay and recovery of K^+ channels in guinea-pig cardiac myocytes. *Am. J. Physiol.* 258:H45–H50.

Tempel, B. L., Y. N. Jan, and L. Y. Jan. 1988. Cloning of a probable potassium channel gene from mouse brain. *Nature* (*Lond.*). 332:837–839

Thuringer, D. and D. Escande. 1990. Apparent competition between ATP and the potassium channel opener RP 49356 on ATP-sensitive K^+ channels of cardiac myocytes. *Mol. Pharmacol.* 36:897–902.

Trube, G., and J. Hescheler. 1984. Inward-rectifying channels in isolated patches of the heart cell membrane: ATP-dependence and comparison with cell-attached patches. *Pflugers Arch.* 407:178–184.

Weston, A. H., and A. Abbott. 1987. New class of antihypertensive acts by opening K^+ channels. *Trends Pharmacol. Sci.* 8:283–284.

Zilberter, Y., N. Bernashev, A. Papin, V. Portnov, and B. Khodorov. 1988. Gating kinetics of ATP-sensitive single potassium channels in myocardial cells depends on electromotive force. *Pflugers Arch.* 411:584–589.